

# Thrust Reverser Effects on Fighter Aircraft Aerodynamics

A. Glezer,\* R.V. Hughes,† and B.L. Hunt‡  
Northrop Corporation, Hawthorne, California

Wind tunnel studies were conducted using a 0.025 scale model of an F-18 type of configuration with thrust reversers in the Northrop 21 × 30 in. low-speed wind tunnel at conditions representative of the aircraft on approach. A feature of these tests was a systematic buildup of reverser jets and tail surface components in order to identify and understand the major aerodynamic forces that the reversers generate on the tail surfaces. It is shown that the upper jets produce a blockage between the twin vertical tails and that this plays a key role in the reverser-induced effects. In sideslip or with the rudders deflected, this blockage is asymmetric and results in increases in directional stability and rudder effectiveness. In pitch, the blockage produces a download on the vertical tails but the resulting upwash on the horizontals greatly reduces the incremental pitching moment on the aircraft. The reverser jets induce a strong entrainment flow on the horizontal tails, which amplifies the tail load, resulting in either a pitch-up or a pitch-down, depending on the tail setting.

## Nomenclature

$b$	= wing span
$\bar{c}$	= wing chord
$C_L$	= lift coefficient
$C_m$	= pitching moment coefficient for a moment center at $0.25\bar{c}$
$C_{m0}$	= $C_m$ at $C_L = 0$
$C_{m\delta_H}$	= increment in pitching moment per degree of horizontal tail deflection
$C_n$	= yawing moment coefficient for a moment center at $0.25\bar{c}$
$C_{n\delta_r}$	= increment in yawing moment per degree of deflection of both rudders
$C_p$	= pressure coefficient, $(p - p_0)/q_0$
$p$	= static pressure
$p_0$	= freestream static pressure
$q_j$	= jet dynamic pressure evaluated for ideal expansion of the jets to freestream static pressure
$q_0$	= freestream dynamic pressure
$q_r$	= dynamic pressure ratio, $q_j/q_0$
$r$	= radial distance
$\alpha$	= angle of attack
$\beta$	= angle of sideslip
$\Delta C_m$	= $C_m(q_r) - C_m(0)$
$\delta_H$	= horizontal tail deflection angle
$\delta_r$	= rudder deflection angle
$\theta$	= cant angle of vertical tails

## Subscripts

$V$	= vertical tail
$WB$	= wing/body

## Superscripts

$L$	= left vertical tail
$R$	= right vertical tail

## Introduction

THE ability to operate from bomb-damaged runways is very likely to be required of future fighter systems because of the vulnerability of airfields near the battle area.

Received April 18, 1984; revision received Feb. 2, 1985. Copyright © American Institute of Aeronautics and Astronautics, Inc., 1985. All rights reserved.

\*Senior Engineer, Propulsion Research Department, Aircraft Division.

†Engineering Specialist, Aerosciences Test and Operations Department, Aircraft Division.

‡Manager, Aerosciences Technology, Aircraft Division. Associate Fellow AIAA.

As argued in Ref. 1, the most critical problem occurs on landing because conventional fighter aircraft require landing distances on wet runways that are several times their takeoff distances. References 1 and 2 show that a thrust reverser is a strong candidate as a solution to the problem if it is used on approach as well as on the ground. The reduced landing field length comes from two factors: deployment on approach allows the engine to be maintained at intermediate power, thus avoiding spool-up delay after touchdown; and reverser modulation gives a more precise control over thrust and hence over the approach flight path, thus enabling the dispersion on the touchdown point to be reduced.

Previous experience of approach and landing thrust reversers indicates that the reversers can cause a serious potential problem by interfering with the aerodynamic characteristics of the aircraft, particularly the tail surfaces.<sup>1</sup> The work reported here is part of Northrop's on-going efforts to understand the problem and develop solutions. Previously reported studies<sup>1,2</sup> were conducted on a twin-engined advanced fighter with a single vertical tail. These results showed that, for this configuration, the reversers have little effect on longitudinal stability, but they do produce an incremental pitching moment, changes in directional stability, an increase in horizontal tail effectiveness, and a decrease in vertical tail effectiveness. These effects are variously caused by the jets acting as a blockage to the freestream flow over the tails, by entrainment into the jets, and by impingement of the jets directly onto the vertical tail.

The fluid mechanics of these phenomena are complex, configuration dependent, and only partially understood. Some preliminary tests of an F-18 type of configuration (twin vertical tails) suggested that the interaction may be even more complex than for a single vertical tail arrangement. It was therefore decided to conduct a series of wind tunnel tests on an F-18 type model, featuring a careful buildup of the jet and tail surface components in order to identify and investigate the major interaction mechanisms at approach flight speeds. This paper reports these tests and the analysis of the data.

## Test Equipment and Procedure

### Test Apparatus

The tests were conducted using a 0.025 scale model of an F-18 type of configuration in Northrop's 21 × 30 in. low-speed wind tunnel. The facility had been re-equipped and newly commissioned as a tool for rapid, low-cost testing. Because of the newness of the facility and the relatively unusual approach of using such a facility for powered force testing, considerable pains were taken to establish the repeatability and validity of the data.

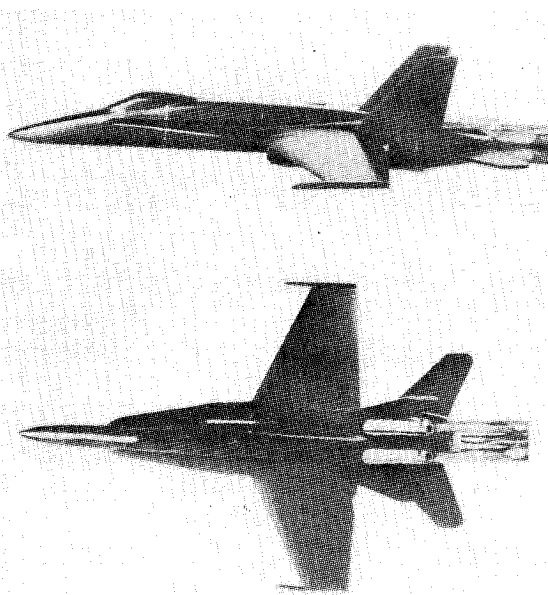


Fig. 1 Wind tunnel model, 0.025 scale.

The 21×30 in. wind tunnel is an open-circuit, ejector-powered tunnel. The test section is a 0.25 scale version of the Northrop Aeronautical Laboratory 7×10 ft low-speed wind tunnel. The model was sting supported via a Task/Able 0.5-in.-diam, six-component internal balance. Data were acquired and reduced on a Cromemco microcomputer.

The 0.025 scale model is illustrated in Fig. 1. It was fabricated using low-cost techniques wherever possible. Construction was from mixed plastic and wood with steel inserts for the balance sleeve and wing and tail attachments. The engine inlets were faired over on the model and the wing flap deflections were zero. The reverser plumes were simulated by means of compressed air jets blown out of four nonmetric convergent nozzles. The nozzles were molded from fiberglass and supplied by 0.34 in. i.d. copper pipes clamped to the sting support system. The pipes and nozzles were laid in slots cut out of the afterbody of the model. With this arrangement of nonmetric nozzles, the thrust forces were not measured, so that the balance sensed directly the aerodynamic forces induced on the airframe by the reversers, these being the forces of interest in this study.

The reverser ports were arranged symmetrically, one above and one below each engine, in the vertical planes through each engine centerline. They were located a distance of  $0.29\bar{c}$  behind the roots of the trailing edges of the vertical tails, where  $\bar{c}$  is the mean aerodynamic chord of the wing. The exits of the ports were square, their size corresponded to full reverse thrust, and they exhausted forward in the vertical plane at 60 deg to the aircraft centerline.

This test arrangement corresponds to a reverse thrust coefficient close to 50%. In practice on approach, the reverser will be at a modulated setting so that there will be exhaust flow from the aft thrust nozzle and the reverser port areas will be approximately 35% of the full reverse thrust areas. The aft thrust nozzle flow was omitted because it is not expected to have much effect on the results and its omission greatly simplified the test. At most, the aft thrust jet may slightly influence the mid-to-far-field trajectories of the reverser plumes, but it is unlikely to greatly alter them in the near field, which is the dominant region for producing the induced effects on the airframe. The effect of the enlarged reverser flows will be to somewhat exaggerate the magnitudes of the reverser-induced effects; the greater area will not change the interaction mechanisms, which were the main object of this investigation. Other data<sup>3</sup> show that the exaggerations in the induced increments are generally around 50%.

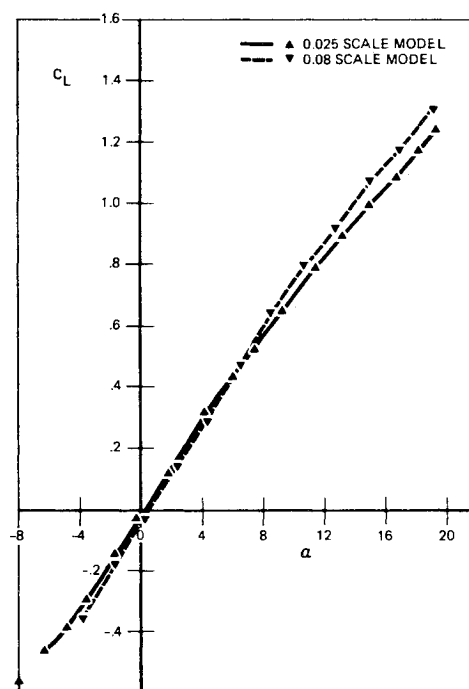


Fig. 2 Comparison of measured lift coefficients for the 0.025 scale model in the 21×30 in. tunnel with lift coefficients for the 0.08 scale model in the 7×10 ft tunnel ( $\delta_H = 0$ , jets off).

#### Test Procedure

The primary parameter used to represent variations in the jet and freestream conditions was the dynamic pressure ratio  $q_r$ , which is the ratio of the dynamic pressure of the jets  $q_j$  to the dynamic pressure of the freestream  $q_0$ . During the approach and landing of an aircraft,  $q_r$  changes due to the changing flight speed at constant nozzle pressure ratio. However, in these tests, variations in  $q_r$  were obtained by varying the nozzle pressure ratio at fixed tunnel dynamic pressure. This procedure allows a much higher rate of data acquisition, hence giving higher data density in a given test time than can be achieved by varying the tunnel speed. Furthermore, other reverser testing at Northrop<sup>3</sup> has shown that the effects of variations in nozzle pressure ratio (NPR) at constant  $q_r$  are small compared to those of  $q_r$  at constant NPR, at least within a range of NPR of 2-4.5.

#### Data Quality

The use of a relatively small and inexpensive wind tunnel and model creates natural concerns for the quality of the data due to the reduced value of the Reynolds number and the accuracy of the model. At the normal operating condition, the Reynolds number in the test section was approximately 900,000/ft, giving typical chordwise Reynolds numbers for the wings and tails of around 240,000 and 131,400, respectively. Although lower than those generally used in aircraft testing, comparisons of the jet-off results from this and subsequent tests with established data bases have shown that, for configurations with thin wings of low-to-moderate aspect ratios, very satisfactory force data and stability and control derivatives can be obtained. For example, Figs. 2 and 3 present comparisons of jets-off data from the current tests with corresponding data from a 0.08 scale F-18 type model tested in Northrop's 7×10 ft low-speed wind tunnel.

Figure 2 shows lift coefficient  $C_L$  as a function of angle of attack  $\alpha$  for the two models, while Fig. 3 presents a comparison of  $C_L$  vs pitching moment coefficient  $C_m$ . The two models differ somewhat in the following details: the 0.08 scale model had flow-through inlets, whereas the 0.025 scale model did not; the leading-edge extension geometries were slightly different; and the 0.025 scale model had slots in the afterbody

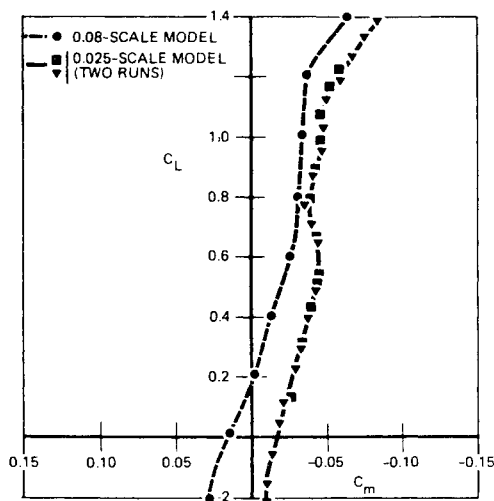


Fig. 3 Comparison of longitudinal stability characteristics for the 0.025 scale model in the 21x30 in. wind tunnel and the 0.08 scale model in the 7x10 ft wind tunnel ( $\delta_H=0$ , jets off).

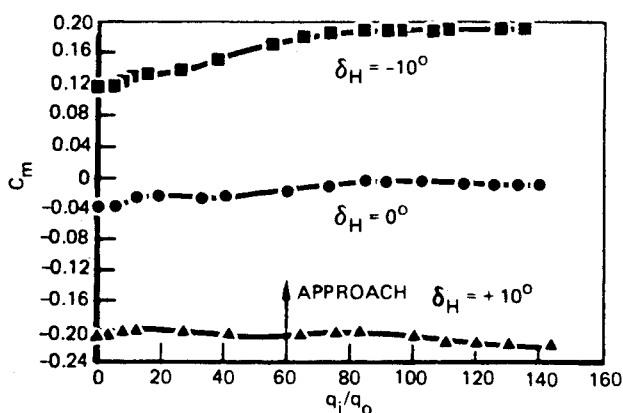


Fig. 4 Reverser-induced pitching moment for three horizontal tail angles ( $\alpha=8$  deg,  $\beta=0$  deg).

and no provision for measurement of cavity pressure. These differences are believed to account for the small differences in the lift data in Fig. 2 and the  $C_{M0}$  shift and slight change in stability seen in Fig. 3. Good agreement was also obtained in tail effectiveness and in aircraft directional characteristics (lateral characteristics were small and not analyzed in detail). The repeatability of the data from the 0.025 scale model was extensively checked and found to be excellent, both jets-off and jets-on. Figure 3 includes two typical repeat runs. Furthermore, the trends in the reverser-induced forces have been confirmed by subsequent tests<sup>3</sup> in the Northrop 7x10 ft wind tunnel using a larger model that was of a generally similar configuration, but that differed in geometric detail.

The possibility that the jets may cause interference by impinging on the tunnel walls and separating the tunnel boundary layers has also been investigated experimentally at Northrop. The results show that there is no impingement for the values of  $q_r$  used here.

### Discussion of Results

This section presents and discusses the test results in two parts. First, the data obtained for the complete aircraft configuration are considered in terms of the aircraft aerodynamic stability and control characteristics. Second, selected results from the systematic model buildup tests are presented and used to identify the aerodynamic mechanisms that are operating and producing the forces measured on the complete configuration.

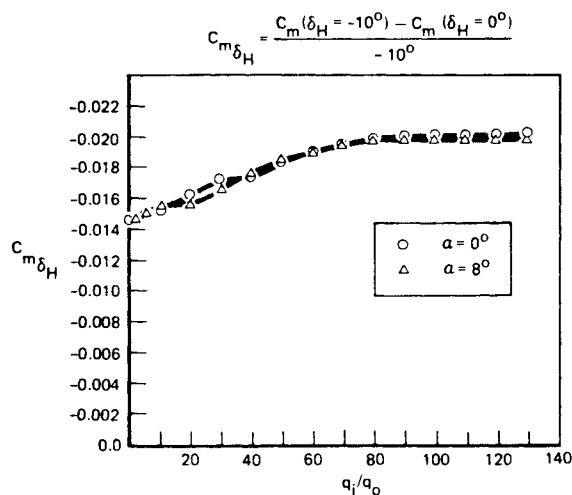


Fig. 5 Effect of reverser jets on horizontal tail effectiveness for two angles of attack.

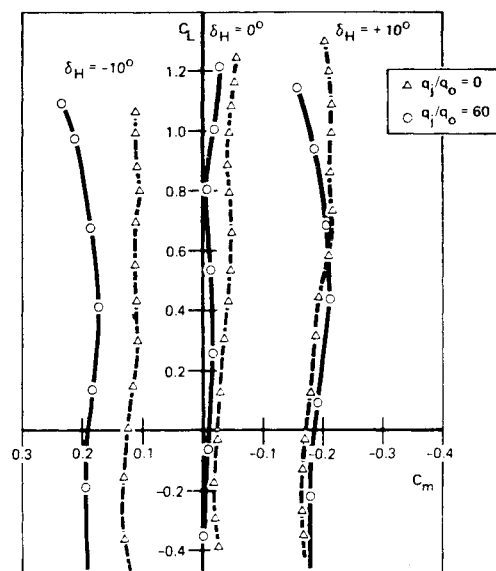


Fig. 6 Effect of reverser jets on longitudinal characteristics.

### Impact on Aircraft Stability and Control

The basic lift and pitching moment characteristics of the model for zero reverser flow can be seen in Figs. 2 and 3. Figure 4 shows the effect of the reversers on the pitching moment at an angle of attack of 8 deg. Reverser and freestream conditions are represented by the dynamic pressure ratio  $q_r$ . It can be seen that some small-amplitude changes in pitching moment occur at low values of  $q_r$ . Such behavior is found to be typical in these tests. Overall, there is only a very small effect on  $C_m$  at  $\delta_H=0$  deg and  $\delta_H=+10$  deg. The changes in  $C_m$  at  $\delta_H=-10$  deg are of moderate magnitudes, corresponding at most to 4.5 deg of equivalent horizontal tail deflection (based on  $C_{m\delta_H}$  at  $q_r=0$ ). However, Fig. 5 shows that  $C_{m\delta_H}$  increases with  $q_r$ , thus decreasing the necessary trim change to 3.5 deg. It can also be seen that  $C_{m\delta_H}$  is almost identical for the two angles of attack  $\alpha=0$  and 8 deg.

Figure 6 shows the effect of the reversers at  $q_r=60$ , which is a typical approach condition, on the longitudinal stability. There is a decrease in stability at typical approach values of  $C_L$  of around 0.6. The change is largest at  $\delta_H=10$  deg, where it corresponds to a forward movement of the aerodynamic center of 0.09 wing chords. The effects at a true trimmed approach condition, with flaps down, may differ.

The reversers induce an increase in the yawing moments due to sideslip (directional stability) and due to rudder deflection

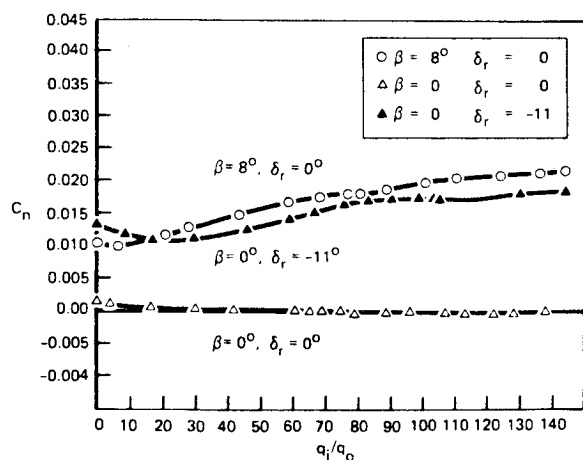


Fig. 7 Effect of reversers on yawing moment for  $\alpha=0$  deg,  $\delta_H=0$  deg.

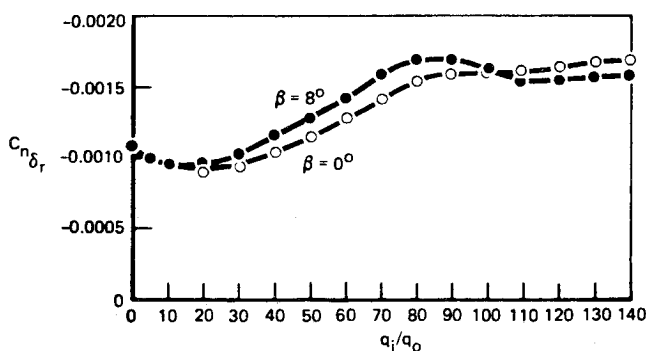


Fig. 8 Effect of reversers on rudder effectiveness for  $\alpha=0$  deg.

(rudder effectiveness) at large values of  $q_r$ , as can be seen in Fig. 7. The increase in yawing moment at 8 deg of sideslip due to blowing at  $q_r=60$  would require 6.2 deg of rudder deflection to trim out this additional yawing moment based on the jet-off rudder effectiveness. In fact, however, the rudder effectiveness is increased by blowing at  $q_r=60$  by an amount that is largely independent of the sideslip angle (see Fig. 8), so that only approximately 2.9 deg of rudder deflection would actually be required. This is a negligible trim change. However, 8 deg corresponds to a cross-wind velocity of only about 18 knots (at an approach speed of 130 knots). At high cross-wind conditions where large rudder deflections are required, the additional yaw moment induced by the reverser may pose a problem requiring particularly careful attention during the integration of the reversers with the airframe.

#### Model Buildup and Identification of Flow Mechanisms

##### Directional Effects

A series of tests was conducted at  $\alpha=0$  deg while varying  $\beta$  between  $-10$  and  $+10$  deg. Systematic buildup of the two vertical tails during these runs led to insight into the aerodynamic mechanisms that produce the incremental stability and rudder effectiveness seen in Figs. 7 and 8. The zero angle-of-attack setting resulted from a constraint in the sting support system. However, low-to-moderate variations in angle of attack were not expected to have a significant influence on the induced directional effects. Subsequent work<sup>3</sup> has shown this assumption to be correct.

Figure 9 shows the yawing moment  $C_n$  measured for each vertical tail in turn and for both verticals at  $\alpha=0$  deg and  $\beta=0$  deg. Forces equal in magnitude and opposite in sign are induced on the verticals. The direction of these forces is such that a positive yawing moment is produced on the left vertical and a negative yaw moment on the right vertical. Thus, the reversers produce outward forces on the vertical tail surfaces.

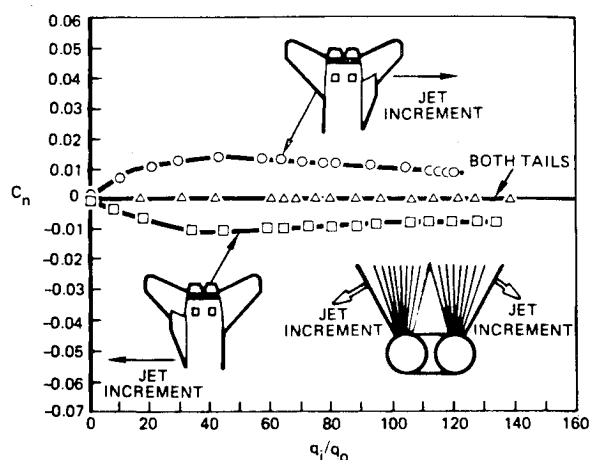


Fig. 9 Buildup of reverser-induced yawing moment ( $\alpha=0$  deg,  $\beta=0$  deg).

To determine the origin of these induced forces, consider the mechanisms through which the reverser jets can affect the airframe. First, they can impinge on airframe surfaces. Second, they induce local velocity changes in the airframe flowfield by acting as solid-body blockages and by entraining external flow through turbulent mixing. These blockage and entrainment effects have been well-established by studies of jets in cross flow and it has been shown that the associated potential flow can be represented analytically by a distribution of doublets and sinks.<sup>4</sup> In the tests described here, the arrangement of jets and the airframe was such that impingement did not occur. This is known to be the case from earlier water tunnel flow visualization and from the absence of condensation or other marks of impingement on the tail surfaces. Now, the flowfields induced in uniform flow by a doublet and by a sink are sketched in Fig. 10. Schematics of the tails are shown by dashed lines. It can be seen immediately that a doublet produces an outward flow angularity, which will create a force on the tail in the outward direction, as measured; on the other hand, the sink creates an inward flow and hence an inward force. Thus, it is clear from the directions of the measured moments that, as far as the vertical tails are concerned, the blockage effect of the jets is dominant.

So far, we have considered only zero sideslip, where the forces on each tail are equal and opposite. Figure 11 shows the yawing moments measured at 8 deg of sideslip. The solid curves in Fig. 11 show the yawing moments on the vertical tails, both individually and in combination, at  $\beta=8$  deg. The moments plotted are increments above the corresponding moments on the wing/body configuration. The dashed curves are the yawing moments measured with one vertical at  $\beta=0$  from Fig. 9 for comparison. It can be seen that the magnitude of the conventional jet-off stabilizing yaw moment for each individual tail is approximately one-half that of the complete configuration. It can also be seen that the jet-induced increment on the left-hand tail is increased by sideslip, while that on the right-hand tail is reduced, resulting in the observed increase in the stabilizing yaw moment on the aircraft. The mechanism believed to cause these changes in sideslip is illustrated in Fig. 12 and discussed in the next paragraph.

Figure 12 is a schematic of the reverser jets and tail arrangement, as seen from the rear. At zero sideslip, the blockage effects of the jets on the twin tails are balanced and there is no net moment on the airplane. In sideslip, however, the jets will move toward the leeward tail and away from the windward tail (because the jets deflect away from the oncoming flow). Thus, the blockage force on the leeward tail will increase, while that on the windward tail will decrease, as observed in Fig. 11. The net induced force thus supplements the aerodynamic restoring force.

The blockage mechanism also explains the increase in rudder effectiveness seen in Fig. 8. As sketched in Fig. 12, deflect-

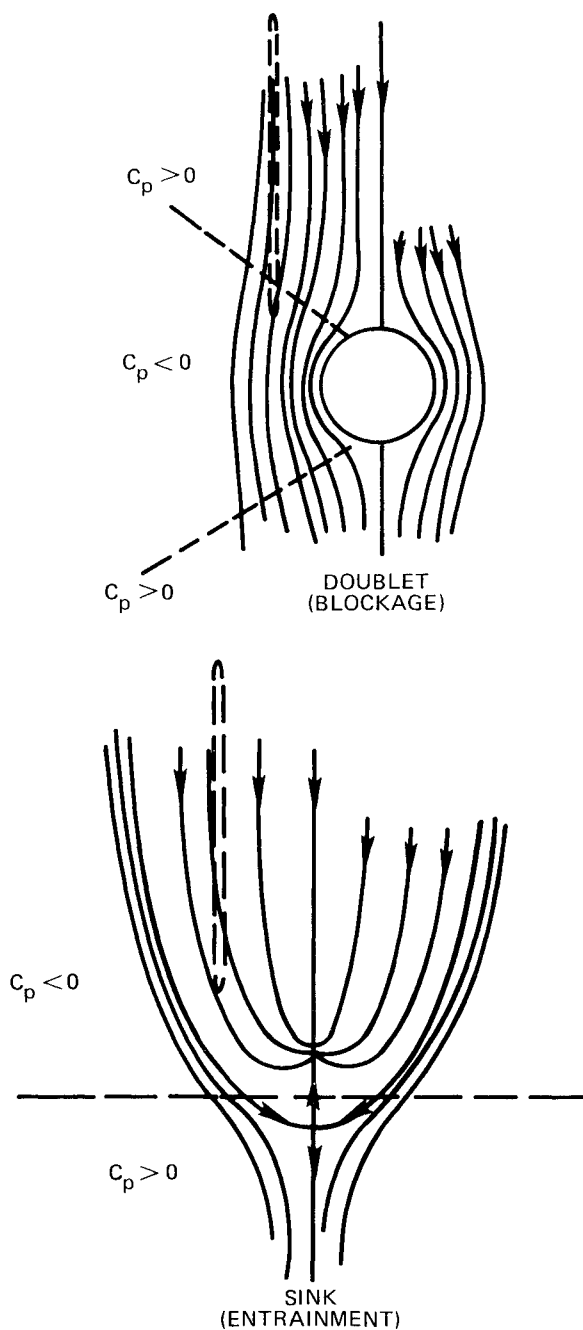


Fig. 10 Flowfields due to a doublet and a sink in cross flow.

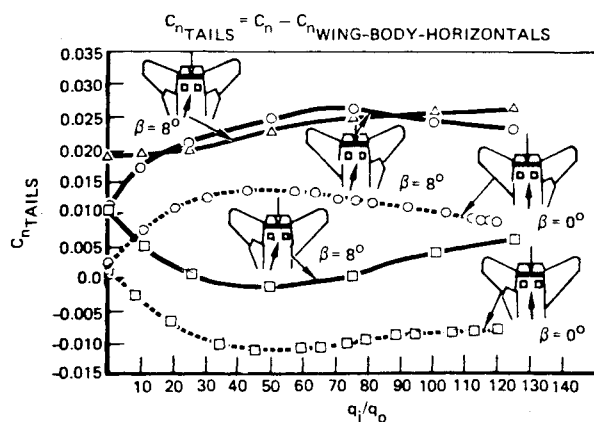
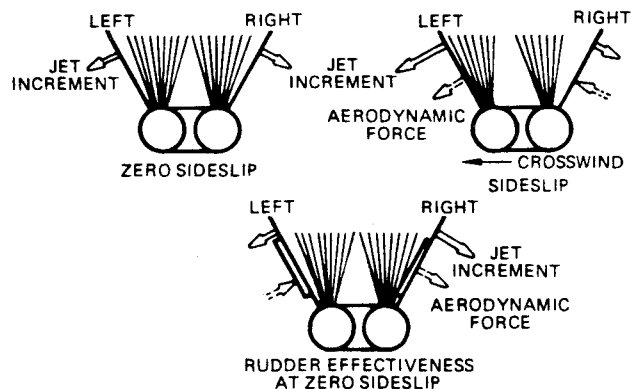
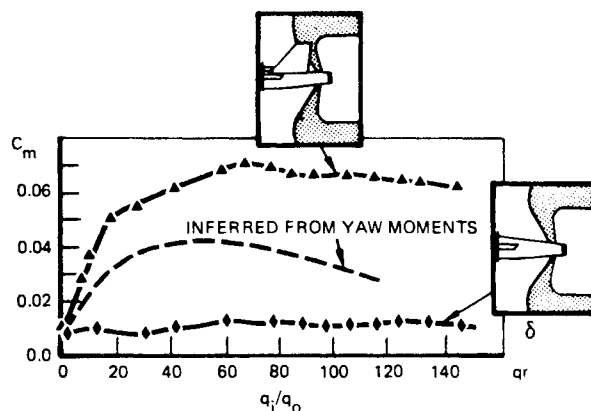
Fig. 11 Reverser-induced yawing moments on vertical tails for  $\alpha = 0$  deg.

Fig. 12 Jet interactions with vertical tails, rear views.

Fig. 13 Pitching moment as a function of  $q$  ratio for wing/body and wing/body/vertical ( $\alpha = 0$  deg,  $\beta = 0$  deg).

ing the rudders brings one rudder surface nearer to the jets while taking the other further away. Again, the resulting net force is in the same direction as the aerodynamic force.

#### Longitudinal Effects

Since the vertical tails are canted 20 deg outward, the yaw moments measured on the individual vertical tails will be associated with a downward force and hence a pitch-up. Figure 13 confirms this effect: it shows the increment in pitching moment due to adding the vertical tails to the wing/body. It can be seen that the wing/body experiences a very small positive pitching moment<sup>§</sup> (which is almost independent of the  $q$  ratio) but, with the addition of the verticals, the jets induce a positive pitching moment equivalent to about 5 deg of jet-off horizontal tail deflection. Data obtained with either the upper or the lower jets operating independently show that this pitch-up is due entirely to the upper jets, consistent with the blockage mechanism sketched in Fig. 12.

The dashed line on Fig. 13 shows pitching moments inferred from the reverser-induced increments in yaw moment contained in Fig. 9. The calculation assumes that the entire jet-induced increments of Fig. 9 occur on the vertical tails. Furthermore, the inferred pitching moments have been made as closely equivalent as possible to the measured wing/body/vertical pitching moments by adding in the (small) jet effect due to the wing/body and referring these combined jet-induced increments to a datum that is the measured jet-off wing/body/

<sup>§</sup>Results obtained subsequently<sup>3</sup> on a larger model having a generally similar tail arrangement with a two-dimensional nozzle afterbody showed a significant reverser-induced pitch-down on the aft fuselage. The absence of a similar moment from the present data is believed to be due partly to the axisymmetric engine nozzles and partly to the afterbody slots in which the reverser supply pipes were located.

vertical pitching moment,  $C_{m_{WBV}}(0)$ . The expressions used to derive the inferred pitching moments are as follows:

$$C_{m_{INF}}(q_r) = C_{m_{WBV}}(0) + \Delta C_{m_{CALC}}(q_r) \\ + C_{m_{WB}}(q_r) - C_{m_{WB}}(0)$$

and

$$\Delta C_{m_{CALC}}(q_r) = \frac{b}{\bar{c}} \tan\{[C_n^L(q_r) - C_n^L(0)] \\ - [C_n^R(q_r) - C_n^R(0)]\}$$

where subscripts WBV and WB refer to data measured on the wing/body/vertical and the wing/body, respectively,  $\theta$  is the tail cant angle,  $b$  the wing span,  $\bar{c}$  the mean aerodynamic chord, and  $C_n^L$  and  $C_n^R$  the yaw moment coefficients from Fig. 9 with the left and right verticals, respectively, in place.

It can be seen that the inferred values are of the same order as those measured, but generally rather smaller. The reason for the discrepancy is not known, but it may be due to the fact that the yaw moment data were obtained with horizontals on, whereas the pitching moments of Fig. 13 were measured with them off. The discrepancy would then represent an upstream effect of the horizontals onto the verticals.

That there is a strong downstream interaction from the verticals onto the horizontals is demonstrated by considering the data of Fig. 14. In this figure, the wing/body/vertical curve of Fig. 13 has been reproduced and contrasted with values obtained for the wing/body/horizontals and for the complete configuration. It can be seen that adding horizontals to the wing/body/verticals reduces the induced pitch-up from about 5 deg of the equivalent horizontal tail deflection to about 1.5 deg. It is natural to suppose that this partial cancellation of pitching moment results from a pitch-down induced by the reversers directly onto the horizontal tails. However, the wing/body/horizontal curve in Fig. 14 shows that the reversers induce essentially no net direct force onto the horizontal tails at this (zero) tail setting. (In itself, this is not surprising since the tail and reverser arrangements are symmetrical.) Therefore, there must be some mutual interaction of verticals, horizontals, and reversers. One candidate hypothesis is that the verticals partially shield the horizontals from the upper jets, thus increasing the relative effect of the lower jets. However, an inspection of Fig. 15 shows that this hypothesis is incorrect, since total removal of the upper jets results in a significant pitch-up at the higher values of the  $q$  ratio (up to 11 deg of equivalent tail deflection), not the pitch-down observed. The correct explanation is believed to be the following. The negative lift on the verticals due to reverser blockage results in an upwash on the horizontals aft of the verticals. The upwash then creates a lift force on the horizontals, which, although smaller than the negative lift on the verticals, generates a nearly equal pitching moment because the moment arm of the horizontals is about twice that of the verticals.

The data of Fig. 15 show that the upper and lower pairs of jets individually induce quite strong pitching moments on the horizontal tails, but that these effects are almost completely balanced when in combination. At small values of the  $q$  ratio, the lower jets produce a pitch-down but this becomes a substantial pitch-up at large  $q$  ratios. The behavior at the higher  $q$  ratios is similar to that observed for a jet exhausting from the under surface of a wing, where a significant downward load is induced.<sup>4</sup> The flow mechanism operating on the wing is believed to act here also: entrainment into the jets creates a strong downwash onto the horizontals, causing the negative lift and consequent pitch-up. The pitch-down at low  $q$  ratios is less easy to explain with confidence. However, surface pressure data for jets in cross flow<sup>5</sup> show that, at low  $q$  ratios, the effect of entrainment into the jet diminishes compared to the effect of blockage. Blockage will create an up-

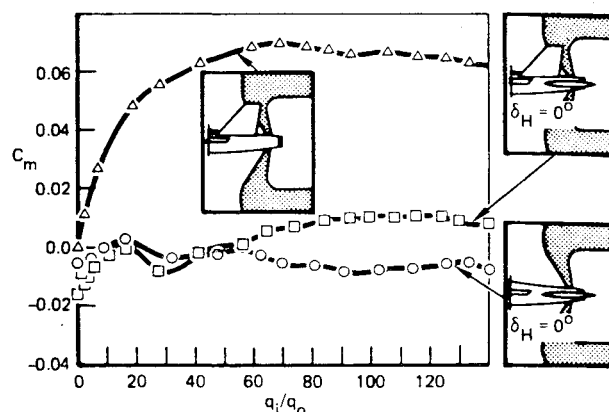


Fig. 14 Effect of horizontal and vertical tails on reverser-induced pitching moment ( $\alpha = 0$  deg,  $\beta = 0$  deg).

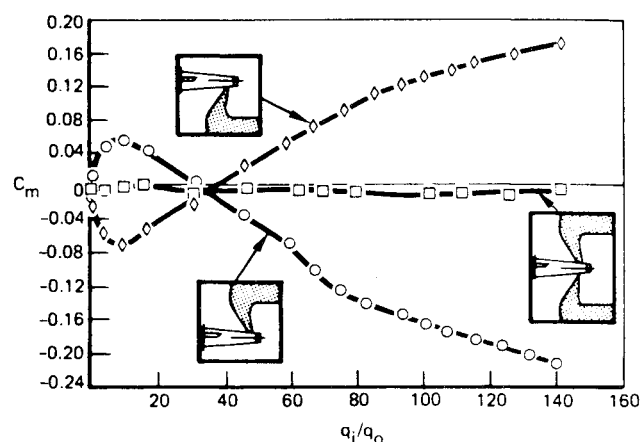


Fig. 15 Pitching moments due to upper and lower jets on the wing/body/horizontals ( $\alpha = 0$  deg,  $\beta = 0$  deg,  $\delta_H = 0$  deg).

wash onto the horizontals and is thus a likely cause of the pitch-down.

At first sight, it may appear inconsistent that, at high  $q$  ratios, the induced effects on the vertical tails are due to blockage, while the effects on the horizontal tails are due to entrainment. However, this is explained by the fact that the vertical tails are much closer to the jets than the horizontals and the effect of blockage (a doublet) falls off as  $r^{-2}$  (where  $r$  is distance from the doublet), whereas the effect of entrainment (a sink) is proportional to  $r^{-1}$ . Blockage is thus felt in the near field of the jets and entrainment in the far field.

Referring to Fig. 4, it can be seen that the effect of the reversers when  $\delta_H = -10$  deg is rather greater than it is when  $\delta_H = 0$  deg. This is believed to result from the entrainment effect of the jets identified from Fig. 15. Entrainment increases the local velocities over the deflected horizontal tails, thus increasing their negative lift and producing the observed pitch-up. There are thus, in total, three mechanisms acting when the horizontal tails have negative deflections: blockage on the verticals (pitch-up), upwash from the verticals onto the horizontals (pitch-down), and entrainment over the horizontals (pitch-up). These three mechanisms are shown schematically in Fig. 16 for a negative tail deflection.

For a horizontal tail setting of  $\delta_H = +10$  deg, entrainment should have the opposite effect to that shown in Fig. 16—it should cause a pitch-down relative to the  $\delta_H = 0$  deg case. The test data confirm this behavior, as illustrated in Fig. 17. In this figure, the pitching moment values of Fig. 4 have been replotted as jet-induced increments. It can be seen that, for moderate and high values of the  $q$  ratio, changing the tail setting from  $-10$  to  $0$  deg and then to  $+10$  deg produces increasingly negative changes in the jet-induced pitching moment, corresponding to the influence of entrainment.

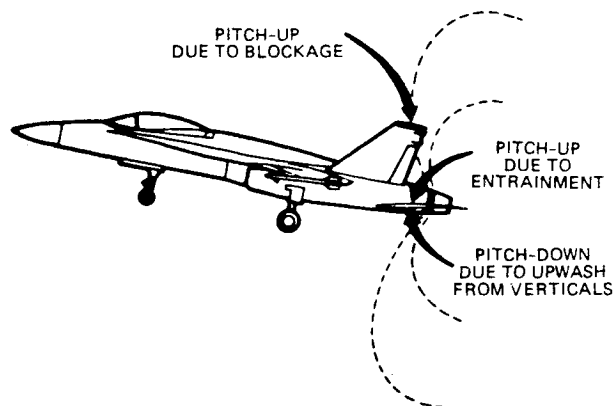


Fig. 16 Mechanisms contributing to longitudinal trim changes for a negative tail deflection.

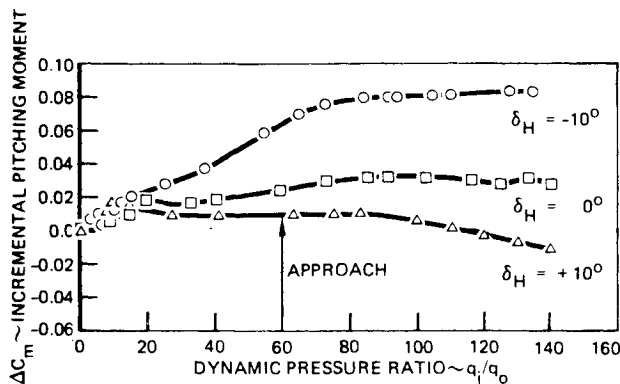


Fig. 17 Reverser-induced increments in pitching moment for three horizontal tail deflections ( $\alpha = 8$  deg,  $\beta = 0$  deg).

### Conclusions

Very repeatable and self-consistent data for the stability and control effects of in-flight thrust reversing have been obtained from a simple test approach. Systematic build up of the tail

and reverser components has enabled the main effects to be explained. The major conclusions from analysis of the data are as follows.

The upper reverser jets produce a blockage between the twin vertical tails that plays a key role in the reverser-induced effects. In sideslip or with the rudders deflected, the blockage effect on the tails is asymmetric and results in increases in directional stability and rudder effectiveness. The resultant effects on the aircraft are small, but need to be carefully investigated when designing for high cross-wind conditions.

In pitch, the blockage-induced loads on the vertical tails act downward, but the resulting upwash onto the horizontal tails greatly reduces the incremental pitching moment on the aircraft. At high  $q$  ratios, the jets induce a strong entrainment flow over the horizontal tails that amplifies the tail load, thus producing either a pitch-up or a pitch-down contribution, depending on the tail setting.

### Acknowledgments

This work was conducted under Northrop's Independent Research and Development Program. The authors very gratefully acknowledge the encouragement, interest, and several key ideas contributed by Dr. Peter Wooler, Technical Director, Northrop F-18 STOL Demonstrator Technology Program.

### References

- <sup>1</sup>Lorincz, D., Chiarelli, C., and Hunt, B.L., "Effect of In-Flight Thrust Reverser Deployment on Tactical Aircraft Stability and Control," AIAA Paper 81-1446, July 1981.
- <sup>2</sup>Chiarelli, C., Lorincz, D., and Hunt, B.L., "Thrust Reverser Induced Flow Interference on Tactical Aircraft Stability and Control," AIAA Paper 82-1133, June 1982.
- <sup>3</sup>Joshi, P.B., "Generic Thrust Reverser Technology for Near Term Application (4 Volumes)," AFWAL Tech. Rept., to be published.
- <sup>4</sup>Wooler, P.T., Burghart, G.H., and Gallagher, J.T., "Pressure Distribution on a Rectangular Wing with a Jet Exhausting Normally into an Airstream," *Journal of Aircraft*, Vol. 4, Nov.-Dec. 1967, pp. 537-543.
- <sup>5</sup>Weston, R.P. and Thames, F.L., "Properties of Aspect Ratio-4 Rectangular Jets in a Subsonic Crossflow," *Journal of Aircraft*, Vol. 16, Oct. 1979, pp. 701-707.